

# Non-perturbative running and renormalization of kaon four-quark operators with $n_f = 2 + 1$ domain-wall fermions

---

**P. A. Boyle, N. Garron\***

*Tait Institute, University of Edinburgh, Edinburgh EH9 3JZ, UK*

**A. T. Lytle\***

*School of Physics and Astronomy, University of Southampton, Southampton SO17 1BJ, UK*

**RBC-UKQCD collaborations**

*Edinburgh 2011/31  
SHEP-1135*

We compute the renormalization factors of four-quark operators needed for the study of  $K \rightarrow \pi\pi$  decay in the  $\Delta I = 3/2$  channel. We evaluate the Z-factors at a low energy scale ( $\mu_0 = 1.145$  GeV) using four different non-exceptional RI-SMOM schemes on a large, coarse lattice ( $a \sim 0.14$  fm) on which the bare matrix elements are also computed. Then we compute the universal, non-perturbative, scale evolution matrix of these renormalization factors between  $\mu_0$  and 3 GeV. We give the numerical results for the different steps of the computation in two different non-exceptional lattice schemes, and the connection to  $\overline{\text{MS}}$  at 3 GeV is made using one-loop perturbation theory.

*The XXIX International Symposium on Lattice Field Theory - Lattice 2011  
July 10-16, 2011  
Squaw Valley, Lake Tahoe, California*

---

\*Speaker.

## 1. Introduction

The RBC-UKQCD collaborations have recently achieved the computation of the  $\Delta I = 3/2$  part of  $K \rightarrow \pi\pi$  decays [1, 2]. At leading order of the operator product expansion, there are three operators that enter the computation : a tree level operator  $Q_1^{3/2}$  and two electroweak penguins  $Q_7^{3/2}$  and  $Q_8^{3/2}$

$$Q_1^{3/2} = (\bar{s}_i \gamma_\mu^L d_i) [(\bar{u}_j \gamma_\mu^L u_j) - (\bar{d}_j \gamma_\mu^L d_j)] + (\bar{s}_i \gamma_\mu^L u_i) (\bar{u}_j \gamma_\mu^L d_j), \quad (1.1)$$

$$Q_7^{3/2} = (\bar{s}_i \gamma_\mu^L d_i) [(\bar{u}_j \gamma_\mu^R u_j) - (\bar{s}_j \gamma_\mu^R s_j)] + (\bar{s}_i \gamma_\mu^L u_i) (\bar{u}_j \gamma_\mu^R d_j), \quad (1.2)$$

$$Q_8^{3/2} = (\bar{s}_i \gamma_\mu^L d_j) [(\bar{u}_j \gamma_\mu^R u_i) - (\bar{s}_j \gamma_\mu^R s_i)] + (\bar{s}_i \gamma_\mu^L u_j) (\bar{u}_j \gamma_\mu^R d_i), \quad (1.3)$$

where  $\gamma_\mu^{R,L} = \gamma_\mu(1 \pm \gamma_5)$  and  $i, j$  are colour indices. In order to simulate a 2-hadron final state with (nearly) physical kinematics and quark masses, the computation of the matrix elements  $\langle \pi\pi | Q_i^{3/2} | K \rangle$  was done on a large volume (of space extent  $L_0 \sim 4.6$  fm), with a rather coarse lattice spacing  $a_0 \sim 0.14$  fm (we refer to this lattice as IDSDR: Iwasaki with Dislocation Suppressing Determinant Ratio, see [3] for more details). The extraction of the bare matrix elements has been reported first last year [4] and updated this year [5]. In this work we explain our method to renormalize non-perturbatively the bare matrix elements computed on this lattice. Since the lattice spacing is rather coarse, the usual Rome-Southampton condition [6] does not hold: in the region where the discretisation effects are under control  $\Lambda_{\text{QCD}}^2 \sim \mu_0^2 \ll (\pi/a_0)^2$ . This problem is circumvented by the use of a step-scaling matrix [7, 8]. Our strategy involves three different steps:

1. We evaluate the Z-factors at low energy  $\mu_0$  on the IDSDR lattice using four different RI-SMOM schemes and compute the relevant renormalized matrix elements. The scale  $\mu_0$  is such that the associated discretisation errors are small but, compared to the Rome-Southampton window, we do not require the non-perturbative effects to be small. Instead one just has to ensure that the finite volume effects are negligible, so the renormalization window becomes

$$L_0^{-2} \ll \mu_0^2 \ll (\pi/a_0)^2.$$

2. We compute the scale evolution between  $\mu_0$  and  $\mu = 3$  GeV of these operators on finer lattices<sup>1</sup> (in practice we use  $a \sim 0.086$  fm, 0.114 fm), on which the high scale lies in the usual Rome-Southampton window

$$\Lambda_{\text{QCD}}^2 \ll \mu^2 \ll (\pi/a)^2.$$

We extrapolate the result to the continuum and obtain the universal running in this energy range for the different renormalization schemes.

3. At the scale  $\mu = 3$  GeV we convert the results to  $\overline{\text{MS}}$  using one-loop perturbation theory [9].

Our strategy - depicted in Fig. 1 - can be summarised by the following equation:

$$\langle O^{\overline{\text{MS}}}(\mu) \rangle = C^{\overline{\text{MS}} \leftarrow \mathcal{S}}(\mu) \times \underbrace{\sigma^{\mathcal{S}}(\mu, \mu_0)}_{\text{Fine lattices } a \rightarrow 0} \times \underbrace{Z^{\mathcal{S}}(\mu_0) \langle O^{\text{bare}}(\mu_0) \rangle}_{\text{Coarse lattice}}, \quad (1.4)$$

<sup>1</sup>We refer to these as the IW(asaki) lattices.

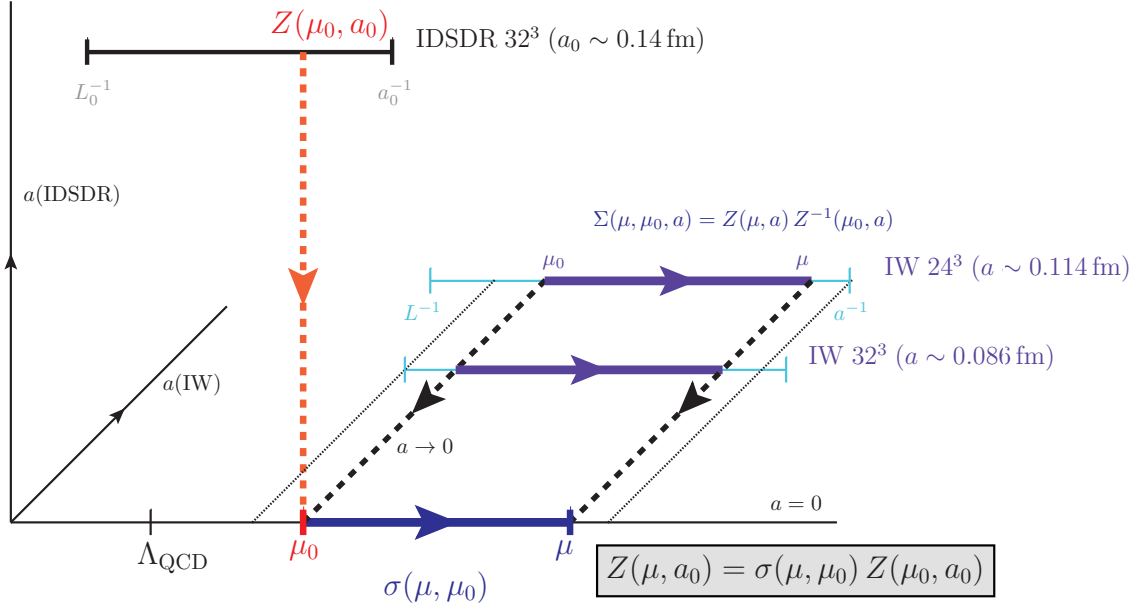


**Figure 1:** Strategy of the renormalization procedure. The horizontal axis represents the energy scale and the two other axes represent the lattice spacings of the IW and IDSDR ensembles. As explained in the text, we compute the renormalization matrix  $Z(\mu_0, a_0)$  at low energy  $\mu_0$  on the coarse IDSDR lattice. There, the usual Rome-Southampton condition  $\Lambda_{\text{QCD}} \ll \mu_0 \ll a_0^{-1}$  does not hold. Thus we combine this result with the continuum non-perturbative scale evolution  $\sigma(\mu, \mu_0)$  extracted from two finer IW lattices and obtain the renormalization factors at a perturbative scale  $\mu$ , where we match to  $\overline{\text{MS}}$ . On each set of lattices the straight line represents (symbolically) the accessible energy range  $L^{-1} \ll \mu \ll a^{-1}$ , where both finite volume and discretisation effects are under control.

where  $C^{\overline{\text{MS}} \leftarrow \mathcal{S}}(\mu)$  represents the matrix of matching factors which converts the  $Z$ -matrix computed in the scheme  $\mathcal{S}$  to the scheme  $\overline{\text{MS}}$ , and  $\sigma^{\mathcal{S}}(\mu, \mu_0)$  is the non-perturbative running matrix in the scheme  $\mathcal{S}$  (see Section 5 for a precise definition). Since at the moment we have only one lattice spacing on the IDSDR lattice, the previous equation will be affected by lattice artefacts (which are estimated), but in principle we could take the continuum limit of  $Z^{\mathcal{S}}(\mu_0) \langle \mathcal{O}^{\text{bare}}(\mu_0) \rangle$  and interpret Eq. (1.4) as a continuum equation. The final result of Eq. (1.4) does not depend on the choice of intermediate schemes  $\mathcal{S}$  (up to truncation errors in perturbation theory). We use four different non-exceptional schemes (but as motivated in [10] we focus only on two schemes) and use the difference to estimate the size of these errors.

The remainder of the text is organised as follows: in the next section we briefly review the RI-MOM renormalization procedure used in our calculations, focusing on recent innovations extending the original proposal of [6]. Section 3 defines precisely our renormalization prescriptions. Section 4 presents our results for the renormalization factors at low energy on the IDSDR lattice in two different schemes. In Section 5 we define the step-scaling function matrix which gives the scale evolution of the operators under considerations and give our numerical results for these two schemes. Final results in the  $\overline{\text{MS}}$  scheme are presented in Section 6, and our conclusions in Section 7.

## 2. Background on RI-MOM

We impose renormalization conditions directly on the lattice using RI-MOM type schemes, as first proposed in [6]. Because the correlation functions are computed using quarks with fixed external momenta, it is advantageous to compute quark propagators using momentum sources [11],  $\eta \sim e^{ipx}$ . This allows the free spatial index of the propagator to be summed at the vertex, greatly improving the signal and resulting in very small statistical errors, even when using relatively few configurations.

We use a modified kinematic setup to that originally proposed in [6], called “non-exceptional” kinematics, in contrast to the original “exceptional” configuration. Instead of using a single external momentum  $p$  with zero momentum inserted at the vertex, one uses quark propagators with external momenta  $p_1$  and  $p_2$  satisfying  $p_1^2 = p_2^2 = (p_1 - p_2)^2$ , with  $(p_1 - p_2)$  inserted at the vertex. This maintains a single renormalization scale, but suppresses channels in which no momentum is flowing, resulting in a stronger suppression of chiral symmetry breaking effects. Details may be found in [12].

Finally, we make use of twisted boundary conditions [7], in which the quark fields pick up an arbitrary phase at the boundary of the lattice. In this way, we can compute quark propagators at arbitrary momentum instead of only at discrete Fourier modes, i.e. if  $q$  represents the quark field then

$$q(x+L) = e^{i\theta} q(x), \quad p = \frac{2\pi}{L}n + \frac{\theta}{L}. \quad (2.1)$$

There are several reasons for using twisted boundary conditions. The principal motivation is that the direction of  $p$  can be chosen to remain constant as its magnitude and the lattice spacing are changed. *This implies the existence of the continuum limit of the non-perturbative running for all the different momenta.* For a given discretization, all lattice artifacts have a fixed parametric dependence on the renormalization scale. Not only will the resultant data be very smooth in  $(ap)^2$ , it means that data from different lattice spacings lie along a continuum trajectory. They are also practical advantages: we can simulate the same physical scale  $\mu_0$  on both the IDSDR and the IW ensembles (as long as we know the lattice spacings with sufficient precision). Also we do not need to subtract perturbatively the O(4)-lattice artefacts, or to give any more-or-less arbitrary prescription to choose our momenta. Thus the use of twisted boundary conditions forms an essential part of our calculation.

## 3. Renormalization in RI-SMOM schemes

In [10],  $B_K$  was renormalized in four different RI-SMOM schemes. Here we generalise this procedure to the case of operator mixing. The operator  $Q_1$  belongs to the  $(27, 1)$  representation of  $SU(3)_L \times SU(3)_R$ , whereas  $Q_7$  and  $Q_8$  belong to  $(8, 8)$ . Thus, if chiral symmetry is realised, the renormalization pattern is the following (in order to simplify the notations we drop the super-

script 3/2):

$$Q_1^R = Z_{(27,1)} Q_1^{bare} \quad (3.1)$$

$$\begin{pmatrix} Q_7^R \\ Q_8^R \end{pmatrix} = Z_{(8,8)} \begin{pmatrix} Q_7^{bare} \\ Q_8^{bare} \end{pmatrix} = \begin{pmatrix} Z_{77} & Z_{78} \\ Z_{87} & Z_{88} \end{pmatrix} \begin{pmatrix} Q_7^{bare} \\ Q_8^{bare} \end{pmatrix}. \quad (3.2)$$

Moreover the renormalization factors of these operators are related to those of  $\Delta S = 2$  operators relevant for neutral kaon mixing within and beyond the Standard Model, which have been already studied on the lattice (see e.g. [13, 14, 15, 16]). For example  $Z_{(27,1)}$  is the same as  $Z_{VV+AA} = Z_{B_K} Z_A^2$  of [10]. For completeness we repeat here some details of this computation: first we consider the process

$$d(p_1)\bar{s}(-p_2) \rightarrow \bar{d}(-p_1)u(p_2) \quad (3.3)$$

with  $p_1^2 = p_2^2 = (p_1 - p_2)^2 = \mu^2$  for a variety of momenta satisfying this condition. We call  $\Lambda_{\alpha\beta,\gamma\delta}^{ij,kl}$  the corresponding amputated Green function evaluated on Landau gauge-fixed configurations (the colour indices  $i, j, \dots$  and Dirac indices  $\alpha, \beta, \dots$  correspond to the external states). We then have to project this Green function onto its Dirac-colour structure, but since  $\mu \neq 0$  the choice of the projector is not unique. We define two projectors ( $N_C$  is the number of colours):

$$P_{\alpha\beta,\gamma\delta}^{(\gamma^\mu)ij,kl} = \frac{1}{128N_C(N_C+1)} [(\gamma_\mu^L)_{\beta\alpha}(\gamma_\mu^L)_{\delta\gamma}] \delta^{ij} \delta^{kl} \quad (3.4)$$

$$P_{\alpha\beta,\gamma\delta}^{(\not{q})ij,kl} = \frac{1}{32q^2N_C(N_C+1)} [(\not{q}^L)_{\beta\alpha}(\not{q}^L)_{\delta\gamma}] \delta^{ij} \delta^{kl}. \quad (3.5)$$

which act on  $\Lambda$  in the following way:

$$M \equiv P\{\Lambda\} \equiv P_{\alpha\beta,\gamma\delta}^{ij,kl} \Lambda_{\alpha\beta,\gamma\delta}^{ij,kl} \quad (3.6)$$

To renormalize the quark field we use two schemes: the  $\gamma_\mu$ -scheme and the  $\not{q}$ -scheme:

$$Z_q^{(\not{q})} = \frac{q^\mu}{12q^2} \text{Tr}[\Lambda_V^\mu \not{q}] \quad (3.7)$$

$$Z_q^{(\gamma^\mu)} = \frac{1}{48} \text{Tr}[\Lambda_V^\mu \gamma^\mu], \quad (3.8)$$

where  $\Lambda_V^\mu$  is the amputated Green function of the conserved vector current. The renormalization factor  $Z_{(27,1)}^{(A,B)}$  in the scheme  $\mathcal{S} = (A, B)$  is then obtained by imposing

$$Z_{(27,1)}^{(A,B)} = (Z_q^{(B)})^2 [P^{(A)}\{\Lambda\}]^{-1} \quad (3.9)$$

where  $A$  and  $B$  can be either  $\gamma^\mu$  or  $\not{q}$ , in this way we have defined four different non-exceptional RI-SMOM schemes.

For the electroweak penguins we generalise the previous equations to the operator mixing case: they are now two different vertex functions  $\Lambda_7$  and  $\Lambda_8$  and two projectors  $P_7$  and  $P_8$  given by

$$\left[ P_7^{(\gamma^\mu)} \right]_{\alpha\beta,\gamma\delta}^{ij,kl} = [(\gamma_\mu^L)_{\beta\alpha}(\gamma_\mu^R)_{\delta\gamma}] \delta^{ij} \delta^{kl} \quad (3.10)$$

$$\left[ P_8^{(\gamma^\mu)} \right]_{\alpha\beta,\gamma\delta}^{ij,kl} = [(\gamma_\mu^L)_{\beta\alpha}(\gamma_\mu^R)_{\delta\gamma}] \delta^{il} \delta^{jk} \quad (3.11)$$

in the  $\gamma^\mu$  scheme and

$$\left[ P_7^{(\not{q})} \right]_{\alpha\beta,\gamma\delta}^{ij,kl} = \frac{1}{q^2} [(\not{q}^L)_{\beta\alpha} (\not{q}^R)_{\delta\gamma}] \delta^{ij} \delta^{kl} \quad (3.12)$$

$$\left[ P_8^{(\not{q})} \right]_{\alpha\beta,\gamma\delta}^{ij,kl} = \frac{1}{q^2} [(\not{q}^L)_{\beta\alpha} (\not{q}^R)_{\delta\gamma}] \delta^{il} \delta^{jk}. \quad (3.13)$$

in the  $\not{q}$  scheme. Let us call  $M$  the matrix defined by

$$M_{ij}^{(A)} = P_j^{(A)} \{ \Lambda_i \}, \quad (i, j = 7, 8), \quad (3.14)$$

where the projector acts in the same way as in Eq. (3.6). The two by two renormalization matrix  $Z^{(A,B)}$  in the scheme  $\mathcal{S} = (A, B)$  is then defined by

$$Z^{(A,B)} = (Z_q^{(B)})^2 F \left[ M^{(A)} \right]^{-1}, \quad (3.15)$$

where  $F$  is the tree-level value of the matrix  $M$ .

#### 4. Computation of the Z-factors at low energy

As explained in the Introduction, since the extraction of the bare matrix elements is done on the coarse ISDSR lattice, the first step consists in computing the renormalization factors at low energy ( $\mu_0 = 1.145$  GeV) on the same lattice. We follow the procedure described in Section 3 and obtain after a chiral extrapolation

$$Z_{(27,1)}^{(\gamma^\mu, \gamma^\mu)}(\mu_0) = 0.443(01), \quad Z_{(8,8)}^{(\gamma^\mu, \gamma^\mu)}(\mu_0) = \begin{pmatrix} 0.505(01) & -0.114(01) \\ -0.022(03) & 0.231(02) \end{pmatrix}, \quad (4.1)$$

$$Z_{(27,1)}^{(\not{q}, \not{q})}(\mu_0) = 0.489(01), \quad Z_{(8,8)}^{(\not{q}, \not{q})}(\mu_0) = \begin{pmatrix} 0.510(02) & -0.116(01) \\ -0.077(06) & 0.305(04) \end{pmatrix}, \quad (4.2)$$

where the quoted errors are statistical only. Here and in the remainder of this paper we estimate and propagate the statistical errors by using 100 bootstrap samples.

We have done the computation for the four different non-exceptional schemes defined in section 3, but here and in the remainder of the text we choose to quote only the results in the  $(\gamma^\mu, \gamma^\mu)$  and in the  $(\not{q}, \not{q})$ -scheme. In Fig. 2 we show the chiral extrapolation of the renormalization factor  $Z_{11} = Z_{(27,1)}$  in the  $(\gamma^\mu, \gamma^\mu)$ -scheme, evaluated at the scale  $\mu_0$ . Our setup is unitary in the light sector, but the strange quark is partially quenched: we consider only degenerate valence quark masses which are set equal to the sea light quark masses and extrapolated to zero, whereas the sea quark mass of the strange is fixed (to its physical value). As a consequence our results are affected by a small systematic error, which was evaluated in [10] for the  $(27, 1)$  operator.

#### 5. Computation of the non-perturbative running

We now consider two fine Iwasaki lattices, the details of which can be found in [17, 18]. There we compute the renormalization factors following again Section 3. In particular we obtain  $M$  in

the four different RI-MOM schemes (in the following  $M$  can either be a scalar – see Eq. (3.6) – or a matrix – see Eq. (3.14) – depending if we consider the multiplicative renormalization case or the operators mixing case). In order to introduce the step-scaling matrix, we follow [8]: at finite lattice spacing  $a$  and for a given renormalization scale  $\mu$  we consider

$$R_{\mathcal{S}}(\mu, a) = \lim_{m \rightarrow 0} [\Lambda_A^2(\mu, a, m) M^{-1}(\mu, a, m)] , \quad (5.1)$$

and we define the step scaling

$$\sigma^{\mathcal{S}}(\mu, s\mu) = \lim_{a \rightarrow 0} \Sigma^{\mathcal{S}}(\mu, s\mu, a) = \lim_{a \rightarrow 0} [R_{\mathcal{S}}(\mu, a) \times R_{\mathcal{S}}^{-1}(s\mu, a)] , \quad (5.2)$$

(we normalise by  $\Lambda_A^2$  in order to cancel the quark wavefunction renormalization). One important point is that although the quantities  $M$ ,  $Z$  and  $R$  depend on the details of the computation this is not the case for the step scaling matrix which has well-defined continuum limit and is thus universal: it depends only on the choice of the renormalization scheme  $\mathcal{S}$  and on the number of flavours.

When performing the continuum extrapolation, we match scales on the different lattices by interpolating the simulated data, which are very smooth on account of our use of twisted boundary conditions. In the right panel of Fig. 2, we show the step scaling function of the  $(27, 1)$  operators in the  $(\gamma_\mu, \gamma_\mu)$ -scheme at finite lattice spacing and extrapolated to the continuum. Twisted boundary conditions also ensure the data lie along a continuum trajectory, and with two Iwasaki ensembles we attempt to remove the lattice artefacts by doing a linear fit in  $a^2$ . Since we have only two different lattice spacings, we choose to include a (rather conservative) systematic error coming from the difference between the results on our finest Iwasaki lattice and the continuum-extrapolated results. As an example, we show the continuum extrapolation of the  $(8, 8)$  operators in Fig.3. With  $\mu_0 = 1.145$  GeV and  $\mu = 3$  GeV, we obtain:

$$\sigma_{(27,1)}^{(\gamma^\mu, \gamma^\mu)}(\mu, \mu_0) = 0.947(05)(01) , \quad (5.3)$$

$$\sigma_{(8,8)}^{(\gamma^\mu, \gamma^\mu)}(\mu, \mu_0) = \begin{pmatrix} 0.963(06)(14) & 0.376(16)(75) \\ 0.040(19)(20) & 2.174(73)(91) \end{pmatrix} , \quad (5.4)$$

$$\sigma_{(27,1)}^{(\not{q}, \not{q})}(\mu, \mu_0) = 0.881(07)(07) , \quad (5.5)$$

$$\sigma_{(8,8)}^{(\not{q}, \not{q})}(\mu, \mu_0) = \begin{pmatrix} 0.970(08)(08) & 0.288(15)(55) \\ 0.156(37)(46) & 1.855(81)(36) \end{pmatrix} . \quad (5.6)$$

The first quoted errors are statistical, while the second are the systematic from the continuum extrapolation. We remind the reader that these results are universal, they depend on the choice of scheme and on the number of flavours (here  $n_f = 3$ ) but not on the details of the lattice implementation.

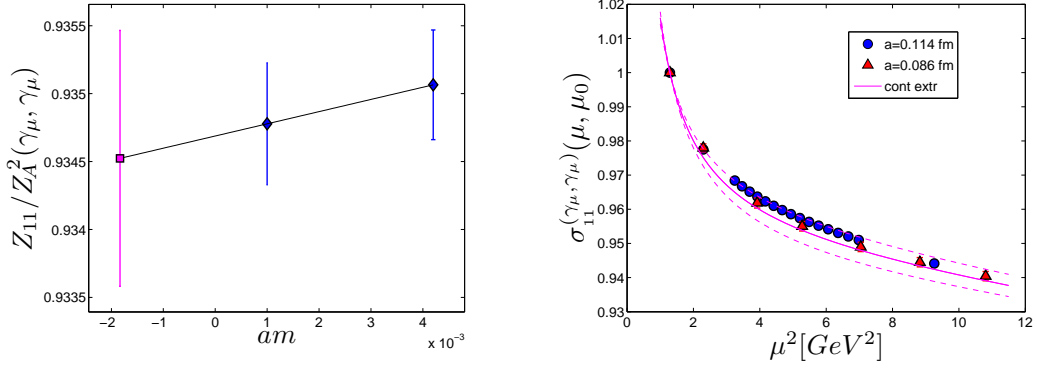


**Figure 2:** The left plot shows the chiral extrapolation of the renormalization factor of the  $(27, 1)$  operator, normalised by  $Z_A^2$ , computed on the IDSDR lattice in the  $(\gamma_\mu, \gamma_\mu)$  scheme. On the x-axis,  $am$  represents the bare light quark mass. We show the result at finite mass and in the chiral limit. On the right we show the non-perturbative scale evolution of the same operator in the same scheme, at finite lattice spacing and in the continuum limit.

## 6. Results in $\overline{\text{MS}}$

The matching to  $\overline{\text{MS}}$  is performed at the scale  $\mu = 3 \text{ GeV}$  where perturbation theory is expected to converge rather well. With  $\alpha_s^{\overline{\text{MS}}}(3 \text{ GeV}) = 0.24544$ , the matching factors are [9]:

$$C_{(27,1)}^{\overline{\text{MS}} \leftarrow (\gamma^\mu, \gamma^\mu)}(3 \text{ GeV}) = 1.00414 \quad (6.1)$$

$$C_{(8,8)}^{\overline{\text{MS}} \leftarrow (\gamma^\mu, \gamma^\mu)}(3 \text{ GeV}) = \begin{pmatrix} 1.00084 & -0.00253 \\ -0.03152 & 1.08781 \end{pmatrix} \quad (6.2)$$

$$C_{(27,1)}^{\overline{\text{MS}} \leftarrow (\not{q}, \not{q})}(3 \text{ GeV}) = 0.99112 \quad (6.3)$$

$$C_{(8,8)}^{\overline{\text{MS}} \leftarrow (\not{q}, \not{q})}(3 \text{ GeV}) = \begin{pmatrix} 1.00084 & -0.00253 \\ -0.01199 & 1.02921 \end{pmatrix}. \quad (6.4)$$

Finally the Z-factors in  $\overline{\text{MS}}$  are given by

$$Z^{\overline{\text{MS}}}(\mu) = C^{\overline{\text{MS}} \leftarrow \mathcal{S}}(\mu) \times \sigma^{\mathcal{S}}(\mu, \mu_0) \times Z^{\mathcal{S}}(\mu_0), \quad (6.5)$$

we obtain:

$$Z_{(27,1)}^{\overline{\text{MS}} \leftarrow (\gamma^\mu, \gamma^\mu)}(3 \text{ GeV}) = 0.421(02)(00) \quad (6.6)$$

$$Z_{(8,8)}^{\overline{\text{MS}} \leftarrow (\gamma^\mu, \gamma^\mu)}(3 \text{ GeV}) = \begin{pmatrix} 0.479(03)(07) & -0.024(04)(17) \\ -0.045(11)(11) & 0.543(18)(23) \end{pmatrix} \quad (6.7)$$

$$Z_{(27,1)}^{\overline{\text{MS}} \leftarrow (\not{q}, \not{q})}(3 \text{ GeV}) = 0.427(03)(03) \quad (6.8)$$

$$Z_{(8,8)}^{\overline{\text{MS}} \leftarrow (\not{q}, \not{q})}(3 \text{ GeV}) = \begin{pmatrix} 0.473(05)(06) & -0.026(05)(17) \\ -0.070(23)(25) & 0.564(27)(13) \end{pmatrix}, \quad (6.9)$$



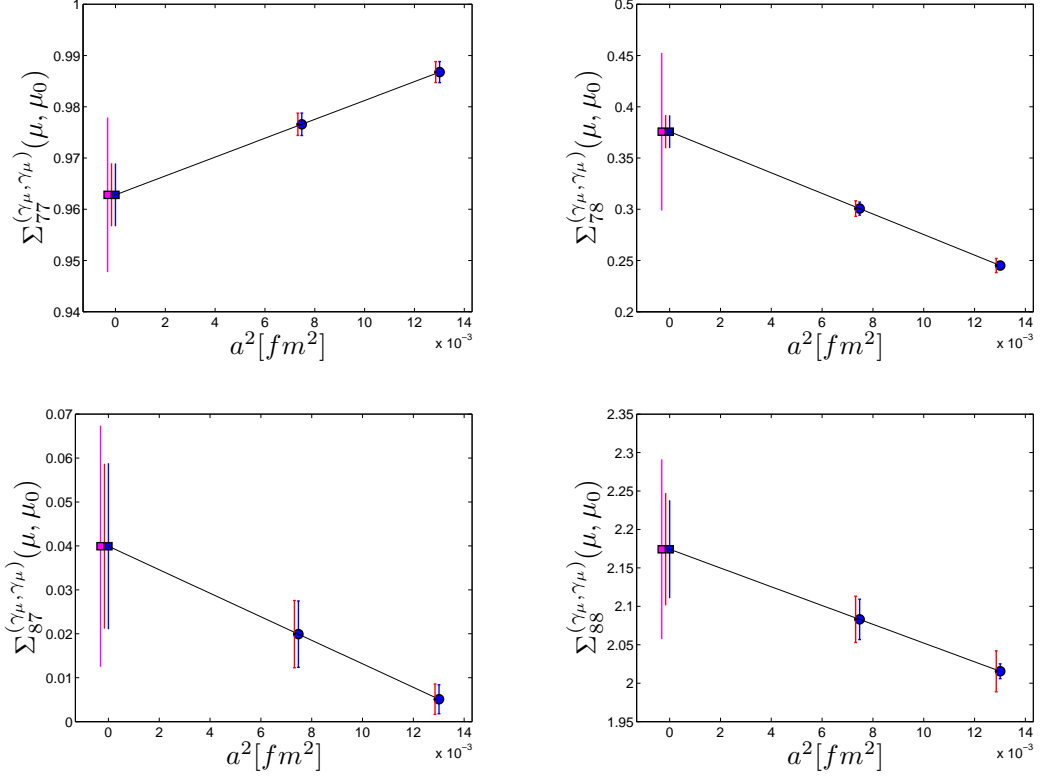


**Figure 3:** Continuum extrapolation of the step scaling matrix elements of the (8,8) operators. At finite lattice spacing we show the central value together with the naive statistical error. Slightly shifted to the left, we show the error bar where we have taken into account the error from the lattice spacing. In the continuum we add in quadrature an error which is defined to be the difference between the continuum extrapolation and the finest lattice spacing; the resulting error is displayed at the far left.

where the first quoted error combines statistical errors, while the second is due to the continuum extrapolation systematic in (5.2). In Eqs. (6.6-6.7-6.8-6.9), the superscript  $\overline{\text{MS}} \leftarrow \mathcal{S}$  reminds us that the  $Z$  factors were first evaluated in the scheme  $\mathcal{S}$ . In principle the results should agree once converted in  $\overline{\text{MS}}$ , but in practice they might be a difference due to lattice artefacts from the IDSDR lattice and due to the truncation of perturbation theory in the conversion to  $\overline{\text{MS}}$ . This difference can be used to estimate the systematic errors or the renormalization procedure.

## 7. Conclusion

We have computed the matching factors required for the determination of the RBC-UKQCD collaborations' recently completed calculation of  $K \rightarrow \pi\pi$  decays in the  $\Delta I = \frac{3}{2}$  channel. The low energy matrix elements were computed on a single, coarse ( $a \sim 0.14$  fm) IDSDR ensemble. In order to make an end-run around the upper limit of the Rome-Southampton window, we have calculated non-perturbative step-scaling functions on IW lattices with smaller lattice spacings ( $a \sim 0.114$  fm and 0.086 fm), and extrapolated them to the continuum. The use of twisted boundary conditions is a crucial element that makes this possible. The end result is that we can apply

the one-loop perturbative SMOM $\rightarrow\overline{\text{MS}}$  matching factors at a scale 3 GeV where perturbation theory converges rather well. The use of multiple intermediate schemes gives an additional useful handle on the effect of truncation at one loop. In the future we plan to apply the same strategy to the  $\Delta I = 1/2$  operators, which require the computation of eye-diagrams. A complete computation of the relevant matrix element for unphysical kinematics has been recently published in [19] and reported at this conference [20].

## Acknowledgements

We warmly thank all our colleagues of the RBC-UKQCD collaborations, and in particular Norman Christ and Chris Sachrajda for suggestions and stimulating discussions, Rudy Arthur and Chirs Kelly for their help at different stages of the project. N.G. is supported by STFC grant ST/G000522/1. A.L. is supported by STFC Grant ST/J000396/1. We thank the STFC funded DiRAC facility (supported by STFC grant ST/H008845/1), the University of Southampton's Iridis cluster (supported by STFC grant ST/H008888/1) and the EU grant 238353 (STRONGnet).

## References

- [1] T. Blum, P.A. Boyle, N.H. Christ, N. Garron, E. Goode, et al. The  $K \rightarrow (\pi\pi)_{I=2}$  Decay Amplitude from Lattice QCD. 2011.
- [2] R. D. Mawhinney. [Pos\(Lattice 2011\) 024](#), 2011.
- [3] C. Kelly. [PoS\(Lattice 2011\) 285](#), 2011.
- [4] Elaine J. Goode and Matthew Lightman.  $\Delta I = 3/2, K\text{to}\pi\pi$  Decays with a Nearly Physical Pion Mass. [PoS\(Lattice 2010\) 313](#), 2010.
- [5] Elaine Goode and Matthew Lightman. Delta I=3/2 K to pi-pi decays with nearly physical kinematics. [PoS\(Lattice 2011\) 335](#), 2011.
- [6] G. Martinelli, C. Pittori, Christopher T. Sachrajda, M. Testa, and A. Vladikas. A General method for nonperturbative renormalization of lattice operators. *Nucl. Phys.*, B445:81–108, 1995.
- [7] R. Arthur and P.A. Boyle. Step Scaling with off-shell renormalisation. *Phys.Rev.*, D83:114511, 2011.
- [8] R. Arthur, P.A. Boyle, N. Garron, C. Kelly, and A.T. Lytle. Opening the Rome-Southampton window for operator mixing matrices. 2011.
- [9] Christoph Lehner and Christian Sturm. Matching factors for Delta S=1 four-quark operators in RI/SMOM schemes. 2011.
- [10] Y. Aoki, R. Arthur, T. Blum, P.A. Boyle, D. Brommel, et al. Continuum Limit of  $B_K$  from 2+1 Flavor Domain Wall QCD. 2010.
- [11] M. Gockeler et al. Nonperturbative renormalisation of composite operators in lattice QCD. *Nucl. Phys.*, B544:699–733, 1999.
- [12] Y. Aoki et al. Non-perturbative renormalization of quark bilinear operators and  $B_K$  using domain wall fermions. *Phys. Rev.*, D78:054510, 2008.

- [13] R. Babich, N. Garron, C. Hoelbling, J. Howard, L. Lellouch, and C. Rebbi.  $K^0$  - anti- $K^0$  mixing beyond the standard model and CP-violating electroweak penguins in quenched QCD with exact chiral symmetry. *Phys.Rev.*, D74:073009, 2006.
- [14] P. Boyle and N. Garron. Non-perturbative renormalization of kaon four-quark operators with nf=2+1 Domain Wall fermions. *PoS(Lattice 2010)* 307, 2010.
- [15] P. Dimopoulos et al.  $K^0 - \bar{K}^0$  Mixing Beyond the SM from Nf=2 tmQCD. *PoS(Lattice 2010)* 302, 2010.
- [16] J. Wennekers. Neutral Kaon Mixing Beyond the Standard Model from 2+1 Flavour Domain Wall QCD. *PoS(Lattice 2008)* 269, 2008.
- [17] Y. Aoki et al. Continuum Limit Physics from 2+1 Flavor Domain Wall QCD. 2010.
- [18] C. Allton et al. Physical Results from 2+1 Flavor Domain Wall QCD and SU(2) Chiral Perturbation Theory. *Phys.Rev.*, D78:114509, 2008.
- [19] T. Blum, P.A. Boyle, N.H. Christ, N. Garron, E. Goode, et al.  $K$  to  $\pi\pi$  Decay amplitudes from Lattice QCD. 2011.
- [20] Qi Liu. Practical methods for a direct calculation of  $\Delta I = 1/2$   $K$  to  $\pi\pi$  Decay. *PoS(Lattice 2011)* 288, 2011.